

Reactivity Studies of Bipyridine-Ligated Nickel(I) and Nickel(0) Complexes Inform the Mechanism in Modern Cross-Coupling Reactions

T. Judah Raab and Abigail G. Doyle*



Cite This: <https://doi.org/10.1021/jacs.5c11247>



Read Online

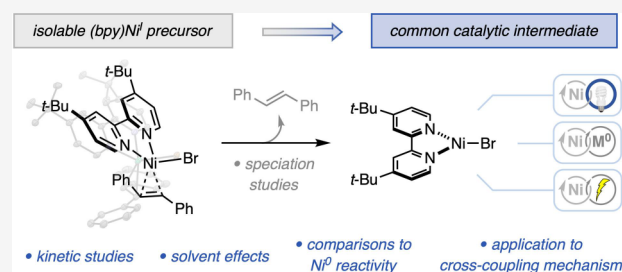
ACCESS |

Metrics & More

Article Recommendations

Supporting Information

ABSTRACT: Bipyridine-ligated nickel(I) and nickel(0) intermediates are widely proposed in Ni-catalyzed cross-coupling reactions. However, few isolable Ni^I and Ni⁰ complexes with catalytically relevant bipyridine ligands are known, limiting our understanding of these complexes' speciation and reactivity. In this work, we identify and investigate well-defined, isolable (^t-Bu₂bpy)Ni^I and (^t-Bu₂bpy)Ni⁰ complexes to characterize their behavior in catalytic systems. Employing spectroscopic and stoichiometric studies, we identified a solvent dependence on rates of the irreversible dimerization of (^t-Bu₂bpy)NiBr, measured rates for the activation of aryl halides and alkyl halides by (^t-Bu₂bpy)Ni^I and (^t-Bu₂bpy)Ni⁰, and found that the reduction of (^t-Bu₂bpy)NiBr to Ni⁰ is inefficient with common heterogeneous metal reductants. Taken together, these studies enable us to propose a general mechanism for cross-electrophile coupling reactions.



1. INTRODUCTION

Recent developments in nickel catalysis have enabled new strategies for the formation of C–X and C–C bonds and expanded the compatibility of sought-after C(sp³)-hybridized substrates in cross-coupling.^{1–3} These modern nickel-catalyzed cross-coupling reactions often leverage Ni's propensity to form open-shell species (e.g., Ni^I and Ni^{III}) to generate and react with carbon-centered radicals. Facile access to these odd-electron Ni species allows for the combination of one- and two-electron elementary steps within a catalytic cycle, underpinning the success of Ni/photoredox, Ni/electrocatalysis, and cross-electrophile coupling (XEC) methodologies.

Despite many advances in reaction development, the mechanisms by which these reactions proceed remain contested. For example, for an established reaction class, C(sp²)–C(sp³) coupling, and the prevalent 2,2'-bipyridine (bpy) ligand scaffold, product formation is well-understood to occur following alkyl radical addition to a (bpy)Ni^{II}(Ar)X species (Figure 1A).^{3–6} However, the reactivity of the resulting (bpy)Ni^IX species is poorly understood: it is commonly proposed that these Ni^I species are reduced to Ni⁰, but recent studies suggest that (bpy)Ni^IX complexes can react with common substrates or irreversibly aggregate (Figure 1B).^{7–10} Further studies on the reactivity of catalytically relevant low-valent Ni complexes are necessary to better understand the elementary steps that are key to modern Ni-catalyzed cross-coupling reactions, which will enable practitioners to boost reaction efficiency and selectivity, aid in the development of

new methods, and improve the performance of data-driven modeling in this area.¹¹

Efforts to study (bpy)Ni^IX complexes directly have yielded conflicting results, with data obtained from well-defined, isolable complexes contrasting with observations of (bpy)Ni^IX species generated in situ. These discrepancies are likely due to the same properties that confer catalytic activity: (bpy)Ni^IX intermediates are highly reactive and thus prone to deactivation pathways (e.g., aggregation) and redox events (e.g., comproportionation and disproportionation) that complicate their direct study. For one of the most widely used ligands in Ni-catalyzed cross-coupling, 4,4'-di-*tert*-butyl-2,2'-bipyridine (^t-Bu₂bpy), Hazari and co-workers isolated and structurally characterized [(^t-Bu₂bpy)NiCl]₂, which was found to remain dimeric in solution and was unreactive toward aryl iodides.⁷ By contrast, monomeric (^t-Bu₂bpy)NiCl generated in situ by Hadt and co-workers was shown to activate much less reactive aryl chlorides (Figure 1C).⁸ The lack of a well-defined and isolable (bpy)Ni^IX complex with properties consistent with catalytic reactivity has prevented a full understanding of these species' speciation and reactivity in cross-coupling.

Received: July 2, 2025

Revised: August 26, 2025

Accepted: September 3, 2025

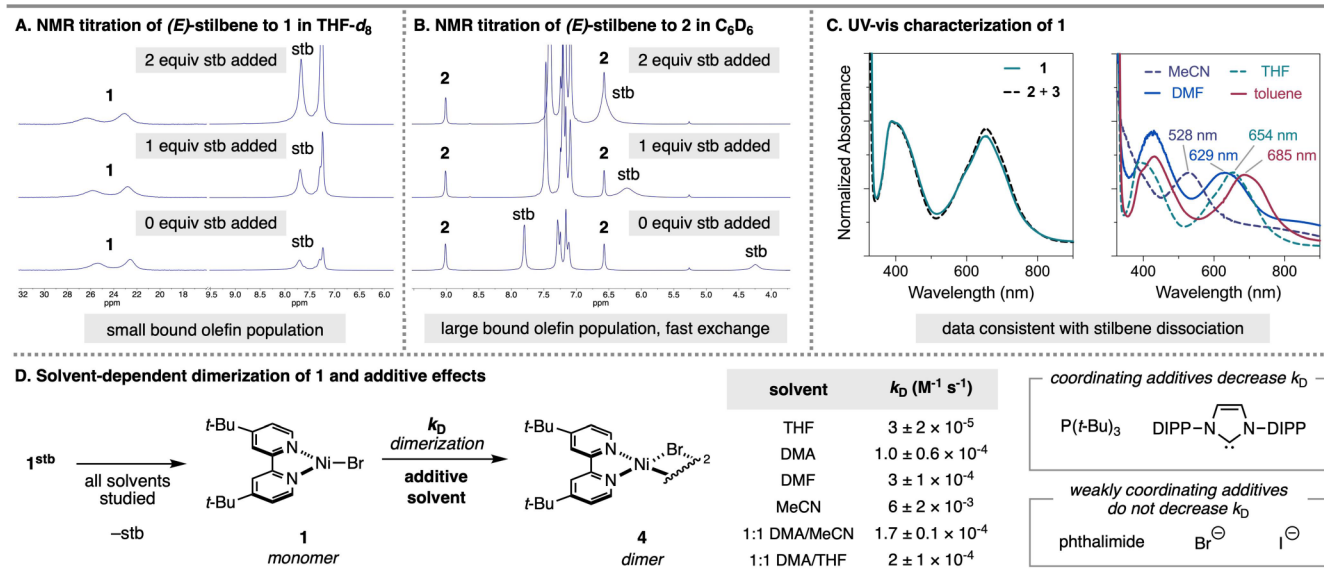


Figure 3. (A, B) ¹H NMR titration experiments evaluating (*E*)-stilbene binding for 1 and 2. UV-Vis characterization of 1 recorded at 23 °C. Left: overlay of a THF solution of 1^{stb} and a 1:1 mixture of 2 and 3 in THF. Right: overlaid spectra of 1 in several organic solvents. λ_{\max} values of the lowest-energy transitions are provided for each solvent. (D) Reaction scheme and evaluation of dimerization of 1 to give 4 across catalytically relevant solvent systems and additive effects. Rate constants measured at 23 °C. Reported standard errors are propagated from the linear least-squares analysis. DIPP = 2,6-diisopropylphenyl.

was isolated as black crystals from a THF/pentane solution in 46% isolated yield (Figure 2B).

Room-temperature EPR spectroscopy of 1^{stb} in THF affords an observed g_{iso} value of 2.211, consistent with the complex's unpaired electron being metal-centered rather than ligand-centered.^{20,22} The ¹H NMR spectrum of 1^{stb} in THF-*d*₈ is characterized by broad resonances, also consistent with the system's unpaired electron. Two resonances appear far downfield—at 25.4 and 22.6 ppm—which we assign as the arene protons of the *t*-Bu^{bpy} ligand. Notably, no resonances consistent with 2 are present, which has been previously observed for a (bpy)Ni^IX complex that is in redox equilibrium with Ni⁰ and Ni^{II} species.⁹

To investigate (*E*)-stilbene binding, we first performed ¹H NMR titration experiments (Figure 3A,B).^{23,24} When additional equivalents of (*E*)-stilbene were added to a THF-*d*₈ solution of 1^{stb}, no shifts were observed in the (*E*)-stilbene protons' resonances, suggesting a large population of unbound (*E*)-stilbene at equilibrium when 1^{stb} is dissolved. In contrast, significant chemical shift changes were observed when (*E*)-stilbene was titrated into a C₆D₆ solution of 2, consistent with a low population of free (*E*)-stilbene and rapid exchange on the NMR time scale.

We next employed UV-vis spectroscopy to further characterize a dark green THF solution of 1^{stb} (Figure 3C). The resulting spectrum features two characteristic bands in the visible region (λ_{\max} values of 388 and 654 nm). Consistent with our observations by ¹H NMR titration, these bands overlap closely with literature spectra for (*t*-Bu^{bpy})NiBr (1) generated in situ.^{8,21,25} Indeed, an identical spectrum was obtained by the comproportionation reaction of 2 with 3, demonstrating that the same species is formed when the (*E*)-stilbene:Ni ratio is <1. We were excited by this result, as the ability to employ 1^{stb} as an isolable source of 1 enabled solvent-dependent and stoichiometric studies that were previously inaccessible via in situ generation.

We began by evaluating the speciation of 1^{stb} in various solvents. UV-vis spectra of 1 in solvents of differing polarity revealed negative solvatochromic behavior (Figure 3C). These shifts are similar to those observed in other bipyridine-ligated metal complexes and are consistent with the previous assignment of these bands as Ni^I-to-bpy metal-to-ligand charge transfer (MLCT) states.^{26,27} In all solvents studied, the MLCT bands of 1 were observed to decay over time, with a particularly rapid decay observed in MeCN.

To assess the species formed, we analyzed a solution of 1^{stb} in CD₃CN by ¹H NMR. Within 15 min, conversion to dimeric [(*t*-Bu^{bpy})NiBr]₂ (4) was observed. Returning to UV-vis analysis, we fit the loss of absorbance at the λ_{\max} of the low-energy band over time in various solvents to determine second-order rate constants for the dimerization of 1 (Figure 3C).²⁸ Notably, the rate at which 1 dimerizes spans multiple orders of magnitude depending on solvent identity, with the fastest rate observed in MeCN ($6 \pm 2 \times 10^{-3}$ M⁻¹ s⁻¹) and the slowest in THF ($3 \pm 2 \times 10^{-5}$ M⁻¹ s⁻¹). The latter value is in good agreement with a previously reported rate constant obtained by Hadt and co-workers following in situ generation of 1 in THF (3.6×10^{-5} M⁻¹ s⁻¹).⁸

The wide range of observed rates and the 10-fold discrepancy between DMF and DMA solutions suggest that solvent coordination influences dimerization kinetics. We therefore evaluated the effect of potentially coordinating additives on the dimerization of 1. Strong σ -donor ligands P(*t*-Bu)₃ and the N-heterocyclic carbene IPr (*N,N'*-1,3-bis(2,6-diisopropylphenyl)imidazol-2-ylidene) rapidly formed 4-coordinate complexes of the type (*t*-Bu^{bpy})(L)NiBr in THF,^{17,18} which were more stable in solution than 1. Previous studies have proposed that the dimerization of (bpy)Ni^IX intermediates in catalysis can also be attenuated by weakly coordinating additives, such as phthalimide and halide additives.^{22,29} In MeCN, we observed no attenuation in the dimerization of 1 in the presence of excess bromide, iodide, neutral phthalimide, or potassium phthalimide, suggesting that

additive binding must be substantial to prevent the formation of **4**.

We have established that the major species in solutions of **1**^{stb} at equilibrium is three-coordinate monomer **1**. In the absence of strong donor ligands, we observe the dimerization of **1** to give **4**, which is most rapid in MeCN. Given the reported recalcitrance of **4** to disaggregation and catalytically relevant reactivity,⁷ we anticipate that our observations will help inform solvent and additive selection for catalytic reactions to prevent formation of deactivated **4**.

2.2. Reactivity with Aryl Halides. With a better understanding of the speciation of **1**^{stb} in solution, we turned our attention to studying its reactivity with catalytically relevant substrates. The oxidative addition of aryl halides to 3-coordinate (bpy)Ni^IX species is invoked as an elementary step in various catalytic reactions, and we have previously observed the oxidative addition of an aryl bromide and an aryl chloride to **1**^{stb} stoichiometrically. The product distribution of this stoichiometric reaction gives a 1:1 ratio of (^t-Bu₃bpy)NiX₂ and (^t-Bu₃bpy)Ni(Ar)X, which is widely proposed to arise via rapid comproportionation of a putative (bpy)Ni^{III}(Ar)X₂ species with remaining (bpy)Ni^IX.^{9,30–32}

To further interrogate the kinetic profile of this reaction, UV–vis spectroscopy was used to monitor the consumption of **1** by the decrease in absorbance at 654 nm (Figure 4A). The reaction of **1** with chloroarenes produced reaction profiles with a first-order dependence on [**1**], and the obtained *k*_{obs} values varied linearly with [ArCl]—indicating a first-order dependence on aryl chloride as well. Consistent with our findings on the solution-phase speciation of **1**^{stb}, no inhibition was observed upon the addition of excess (*E*)-stilbene.

For chlorobenzene, UV–vis analysis gave a second-order rate constant of 0.50 ± 0.01 M⁻¹ s⁻¹, in good agreement with the value reported by Hadt and co-workers for **1** generated in situ (0.41 ± 0.01 M⁻¹ s⁻¹).⁸ Attempts to collect rate data for the reaction of **1** with bromobenzene were hindered by practical limitations, as the reaction was complete within seconds (Figure 5A). We estimate a lower bound of 10² M⁻¹ s⁻¹ for the rate of bromobenzene oxidative addition to **1**, in accord with Bird and MacMillan et al.'s report that iodobenzene reacts with radiolytically generated **1** with a second-order rate constant of 2.2 × 10⁴ M⁻¹ s⁻¹ in DMF.²¹

To further investigate the mechanism of oxidative addition to **1**, we varied the electronic and steric properties of the aryl chloride substrates. A Hammett study using a series of 4-substituted chlorobenzenes yielded a linear plot against σ_p , indicating that the mechanism of oxidative addition was conserved across the chloroarenes studied (Figure 4B). The observed ρ value of +2.2 is most consistent with a concerted oxidative addition or halogen atom abstraction mechanism for activation of the C–Cl bond.^{9,33} This modest electronic dependence is less consistent with electron transfer or an S_NAr-type oxidative addition, which has previously been proposed for the reaction between **1** and aryl chlorides in THF.^{8,34}

The steric profile of the chloroarene was also found to influence reactivity. Introduction of ortho-methyl groups to the chloroarene resulted in a ~5-fold and ~30-fold reduction in rate for 2-chlorotoluene and 2-chloro-*m*-xylene, respectively. Notably, a change in the rate law was observed for 2,6-disubstituted haloarenes (both aryl chlorides and aryl bromides). For these substrates, the reaction became second-order in [**1**], which we attribute to a change in mechanism possibly involving aryl radical generation, as previously

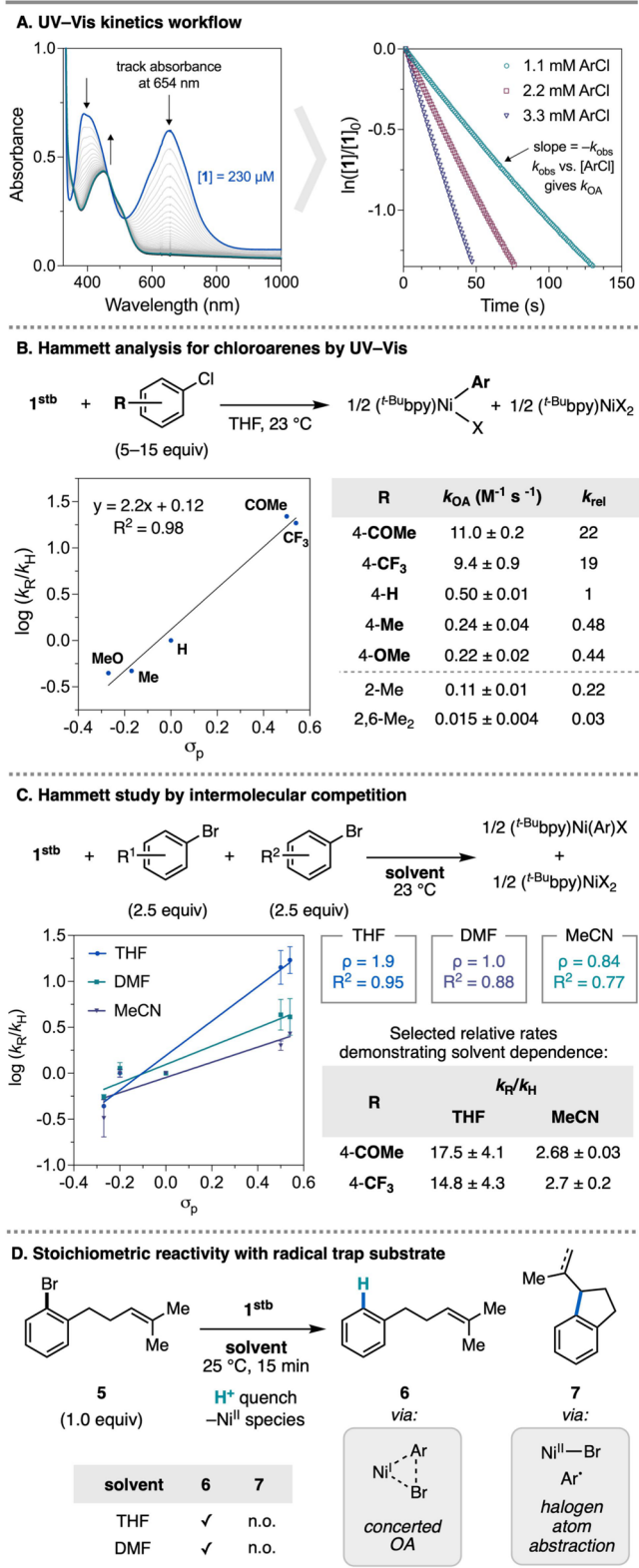


Figure 4. (A) Representative workflow for determining rate constants for oxidative addition to **1**. Reactions were run under pseudo-first-order conditions with respect to [ArCl]. (B) Resulting Hammett plot for a series of chloroarenes. Reported standard errors are propagated from least-squares analysis (Figures S17–S24). (C) Hammett plots generated via competition experiments in different solvents. Error bars are one standard deviation of two trials. (D) Products observed following stoichiometric oxidative addition reactions of radical trap substrate **5**. n.o. = not observed.

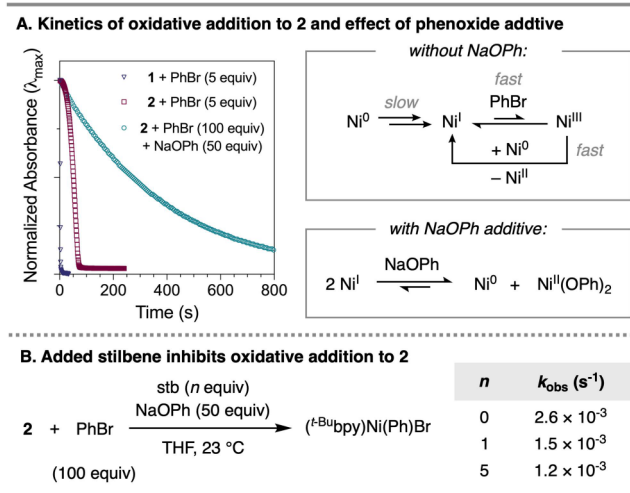


Figure 5. (A) Reactivity comparison between **1** and Ni^0 analog **2** toward PhBr. The sodium phenoxide additive induces disproportionation away from the Ni^I species. (B) Observed rate constants for increasing loading of (*E*)-stilbene in the reaction between **2** and bromobenzene.

observed by Weix and co-workers for hindered aryl iodides (see SI section 5.2 for more discussion).³⁵

We also examined the solvent dependence of aryl halide oxidative addition. Due to the more competitive dimerization pathways in MeCN and DMF, extensive UV–vis studies with aryl chlorides were not conducted in these solvents. Instead, we evaluated product distributions from competition experiments for aryl bromide oxidative addition to **1** to perform a Hammett analysis in DMF, MeCN, and THF.^{36,37} The observed ρ values in the more polar solvents ($\rho = +1.0$ in DMF and $\rho = +0.84$ in MeCN) were smaller in magnitude than the value observed in THF ($\rho = +1.9$). Previously, values of $\rho \sim +1$ for haloarene activation have been attributed to a halogen atom abstraction (XAA) mechanism.³⁸

To probe for this change in mechanism, we prepared an aryl bromide with a pendant olefin (**5**), which was recently shown by Hartwig and co-workers to rapidly cyclize ($k_{\text{cyc}} = 5.8 \times 10^9 \text{ s}^{-1}$) following XAA of the $\text{C}(\text{sp}^2)\text{--Br}$ bond.³⁹ In both THF and DMF, we observed the exclusive formation of the uncyclized product **6** (Figure 4D). While these results are most consistent with a concerted oxidative addition pathway that is independent of solvent, we cannot rule out XAA-type activation followed by rapid in-cage radical recombination with Ni.

Since $(\text{bpy})\text{Ni}^0$ intermediates are also commonly proposed in catalysis, we also evaluated the reactivity of this substrate class with complex **2**. Our first-principles expectation was that the more electron-rich metal center in **2**—in which the olefin ligand undergoes rapid exchange—would undergo oxidative addition with electrophiles more rapidly than **1**. However, treatment of **2** with five equivalents of bromobenzene afforded a reaction profile characterized by a brief induction period followed by a maximum rate slower than that observed for the analogous oxidative addition to **1** (Figure 5A).

We hypothesized that the induction period in the reaction between bromobenzene and **2** may be related to tight binding of the π -system of (*E*)-stilbene. Indeed, the addition of (*E*)-stilbene to the reaction was found to extend the induction period. Furthermore, we postulated that bromobenzene

oxidative addition to **2** may proceed via the intermediacy of **1**, which we demonstrated to undergo this reaction rapidly. To test this hypothesis, we evaluated a sodium phenoxide additive, which is reported to induce disproportionation of $(\text{bpy})\text{Ni}^I\text{X}$ species due to the thermodynamic stability of $(\text{bpy})\text{Ni}^{II}(\text{OPh})_2$.⁴⁰ In the presence of this additive, we no longer observed an induction period, and reaction profiles became first order in [**2**] (Figure 5A).

Unlike the case of aryl halide oxidative addition to **1**, (*E*)-stilbene was found to inhibit the reaction of **2** with bromobenzene (Figure 5B). The rate of reaction with **2** is also several orders of magnitude slower than oxidative addition to **1**, requiring a large excess of bromobenzene to observe the reaction's profile on the order of minutes. Together, these data suggest that (*E*)-stilbene must dissociate prior to oxidative addition to **2**, limiting the relevance of this complex as a Ni^0 analog of **1** in studies of aryl halide reactivity.

However, these findings have interesting mechanistic implications. Clearly, Ni^I species play an important role in the oxidative addition of bromobenzene to **2** in the absence of specific additives. We propose that this reaction proceeds through a radical chain mechanism in which a small amount of Ni^I (likely **1**) formed from **2** reacts with bromobenzene to form a Ni^{III} intermediate, which then comproportionates with **2** to regenerate Ni^I and propagate the chain (Figure 5A). This mechanism is likely to be more accurate than the sequence described above for the synthesis of **1**^{stb} from **2** (Figure 2A). Similar mechanisms are likely operative in reactions that invoke $(\text{bpy})\text{Ni}^0$ intermediates in the presence of olefins—either from Ni precursors (e.g., 1,5-cyclooctadiene (COD) from $\text{Ni}(\text{COD})_2$) or substrates (e.g., an alkene in a dicarbofunctionalization reaction).^{41,42} The apparent generation of **1** from $(\text{bpy})\text{Ni}^0(\text{olefin})$ complexes may also inform precatalyst design: a suitably tuned $(\text{bpy})\text{Ni}^0(\text{olefin})$ precursor could generate **1** in low concentrations, disfavoring off-cycle comproportionation and dimerization pathways that diminish catalytic efficiency.^{29,43}

2.3. Reactivity with Alkyl Halides. With an improved understanding of the reactivity of **1** and **2** with aryl halides in hand, we turned our attention to the activation of $\text{C}(\text{sp}^3)\text{--X}$ electrophiles by these complexes. The generation of alkyl radicals from alkyl halides by low-valent Ni complexes is thought to play an important role in a variety of cross-coupling reactions, most prominently in XECs.^{1,3} It is more frequently proposed that alkyl halide activation occurs from a putative $(\text{bpy})\text{Ni}^I(\text{Ar})$ species rather than $(\text{bpy})\text{Ni}^I\text{X}$, which is based on observations for bisphosphine-bound Ni^I complexes.¹² However, XAA of benzylic chlorides mediated by a (bisoxazoline)- Ni^IX complex has been studied by Reisman and co-workers, suggesting that Ni^IX complexes bearing nitrogen ligands are capable of activating alkyl halides.¹⁵

First, the product distributions resulting from the reaction of a primary alkyl iodide—1-iodo-3-phenylpropane—with **1** and **2**, respectively, were studied (Figure 6A). For both reactions, we observe a mixture of products consistent with the generation of freely diffusing alkyl radicals, with 1,6-diphenylhexane (via radical–radical coupling), *n*-propylbenzene, and 3-phenylpropene observed in both cases. The latter two products are postulated to arise following radical addition to a Ni center, after which protodemetalation in workup would furnish *n*-propylbenzene or β -hydride elimination would give 3-phenylpropene.^{12,44} Only 50% conversion of alkyl halide was observed in the reaction with **1**, similar to observations in the

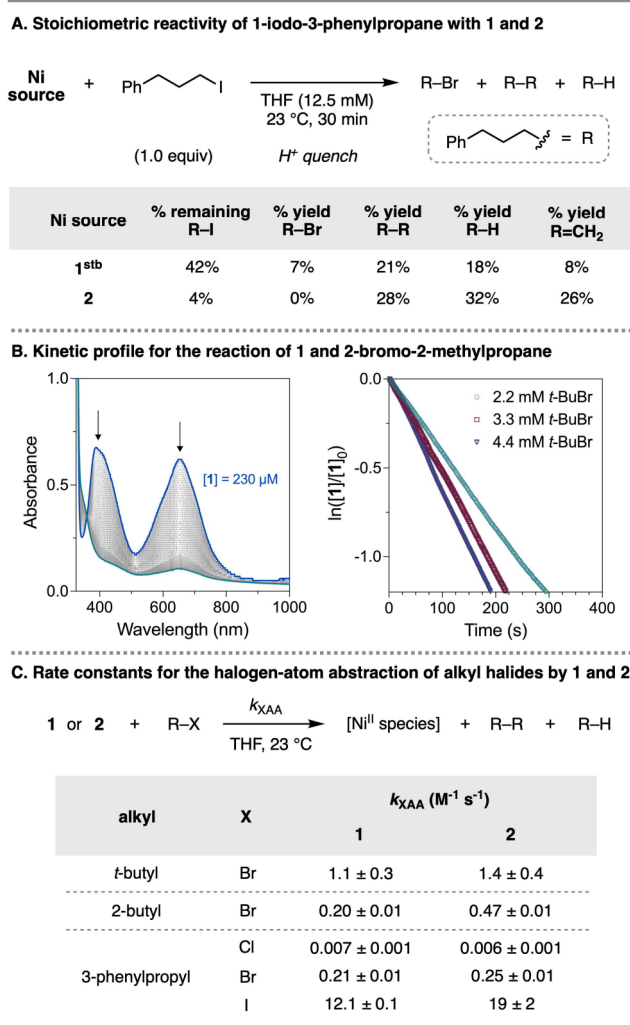


Figure 6. (A) Stoichiometric reactivity of 1-iodo-3-phenylpropane with 1 and 2. Yields were determined by GC. (B) Kinetic profile of the reaction between 1 and 2-bromo-2-methylpropane. (C) Bimolecular rate constants for the halogen atom abstraction of alkyl halides of various substitution by 1 and 2. Reported standard errors are propagated from least-squares analysis (Figures S25–S34).

reaction of 1 with equimolar amounts of aryl halide. In this case, we attribute this additional consumption of 1 to the radical addition pathways. Furthermore, some alkyl iodide is converted to alkyl bromide, suggesting that pathways exist along which alkyl halide activation is reversible.

To compare rates with those of the other reactions studied, we next examined the kinetics of alkyl halide activation by 1 (Figure 6B). In most cases, it was observed that reactions were first order in [1] and first order in [alkyl-X],⁴⁵ allowing for determination of second-order rate constants (Figure 6C). Both halide identity and substitution of the alkyl chain were found to affect rates of activation, with rates for the series of 3-phenylpropyl halides spanning 4 orders of magnitude (I > Br > Cl). Alkyl substitution had a smaller effect on rates of activation, with increasing substitution generally resulting in faster activation (3° > 2° ~ 1°). These observations are consistent with previous studies which invoke a concerted halogen atom abstraction mechanism for alkyl halide activation by low-valent Ni.^{12,16} Interestingly, the rates of halogen atom abstraction (k_{XAA}) observed for alkyl bromides are comparable

in rate with the k_{OA} values reported above for aryl chloride oxidative addition, demonstrating that 1 is better poised to activate C(sp²)-X electrophiles relative to C(sp³)-X electrophiles.

The reactions of alkyl halides with Ni⁰ analog 2 were also investigated. Unlike for the reaction between 2 and aryl halides, no induction period was observed. In all reactions between 2 and alkyl bromides, formation of 1 could be observed at intermediate reaction times, with overlap of absorbance bands complicating UV-vis analysis. In order to track [2], we employed spectral deconvolution by fitting linear combinations of reference spectra of 1 and 2, affording reaction profiles that were first order in [2] (see SI section 8.2 for more details). These observed rate constants for activation at 2 were faster than those for 1 but were of the same order of magnitude in all cases. Similar trends in halide identity and alkyl substitution were observed (I > Br > Cl, 3° > 2° > 1°), consistent with a concerted halogen atom abstraction pathway for alkyl halide activation from 2.

2.4. Reduction of Ni^I to Ni⁰. The reduction of 1 or similar (bpy)Ni^IX species to give (bpy)Ni⁰ intermediates has been proposed in many catalytic reactions, particularly in XECs and metallaphotoredox catalysis.^{3,4} These proposals likely originate from hypotheses that Ni⁰ species are responsible for the activation of various substrate classes in these couplings. However, as demonstrated above, (bpy)Ni^IX species are kinetically competent in reactions with C(sp²)-X and C(sp³)-X electrophiles, which prompted us to assess the feasibility of the reduction of 1 versus its reactivity with electrophiles. Thermodynamic reduction potentials generally support that bipyridine-bound Ni^I/Ni⁰ redox couples are within range of common catalytic reductants,^{4,46} but the inaccessibility of (bpy)Ni^IX complexes has prevented the direct study of these reductions.

With access to 1 upon the dissolution of 1stb, we were able to evaluate reduction reactions with metallic zinc and manganese under XEC-like conditions (Table 1). After heating at 60 °C

Table 1. Reduction of 1 to 2 with Common Heterogeneous Metal Reductants

1 st b		M ⁰ (60 equiv) LiBr (40 equiv)	solvent, 60 °C 1 h		2 + 1/2 MX ₂
solvent	reductant	reducing potential (V vs. Fc/Fc ⁺) ^a	% of active Ni ^b 1	2	
THF	Zn	-1.61 V	92%	8%	
THF	Mn	-1.64 V	69%	31%	
DMF	Zn	-1.53 V	100%	0%	
DMF	Mn	-1.63 V	100%	0%	

^aReducing potentials of Zn/LiBr and Mn/LiBr in THF and DMF from ref 46. ^bFormation of dimer 4 was observed in entries 2–4.

for 1 h, reactions were filtered to remove the reductant and analyzed by UV-Vis spectroscopy to determine the identity of remaining Ni. For Zn or Mn in THF, some formation of 2 was observed, which we attribute to reduction and trapping by free (*E*)-stilbene. Notably, in DMF—a common solvent for XEC reactions—no formation of 2 could be observed for either reductant. These observations demonstrate that the reduction of (bpy)Ni^IX species to (bpy)Ni⁰ by Zn and Mn is inefficient

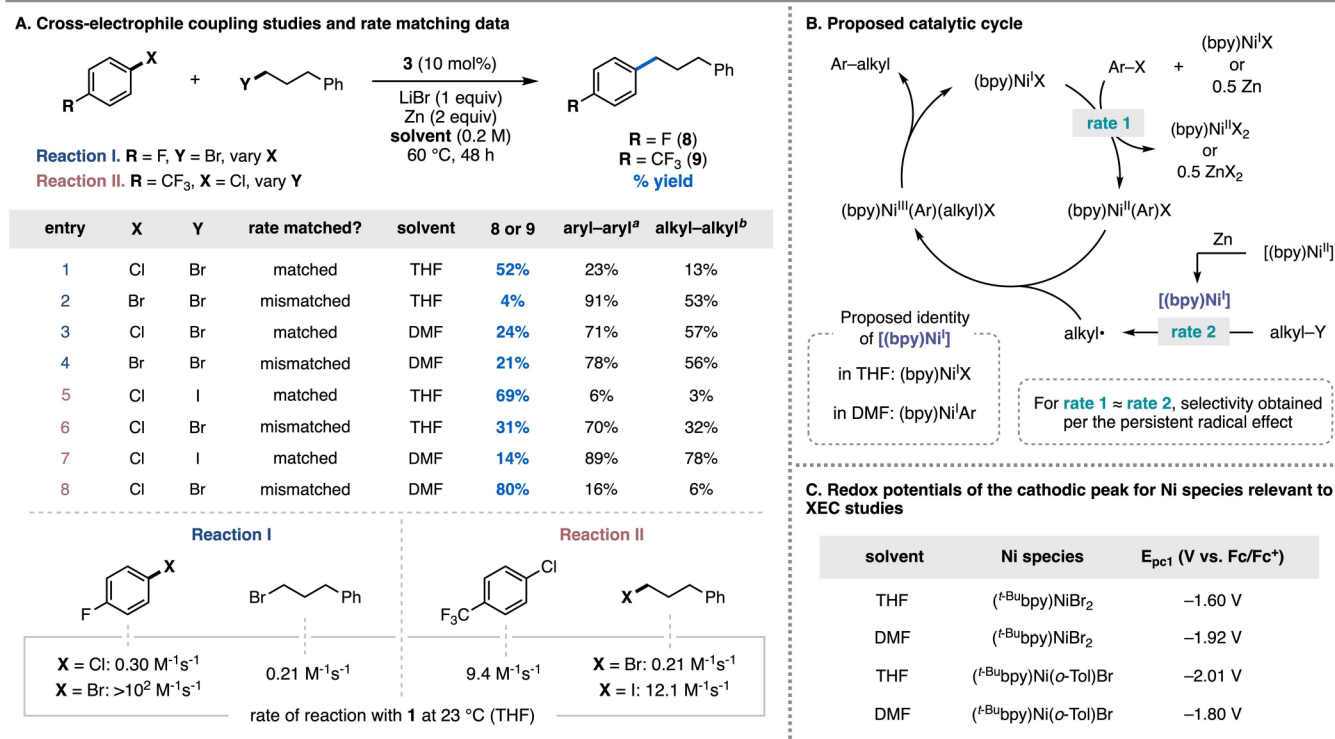


Figure 7. (A) Cross-electrophile coupling studies varying substrate and solvent identity to probe matched/mismatched XECs. (B) Proposed catalytic cycle most consistent with our experimental data. (C) Redox potentials of Ni species relevant to the XEC studies. Yields were determined using ¹⁹F NMR or GC. ^a4,4'-difluorobiphenyl for Reaction I, 4,4'-bis(trifluoromethyl)biphenyl for Reaction II. ^b1,6-diphenylhexane.

under XEC conditions relative to reactions of (bpy)Ni^IX with electrophiles.

2.5. Using Observed Reactivity to Investigate the Cross-Electrophile Coupling Mechanism. With an improved reactivity profile of **1** in hand, we hypothesized that our findings would allow for an investigation of the mechanism and origin of cross-selectivity in C(sp²)-C(sp³) XEC reactions. Our observations that reactions between **1** and XEC electrophiles proceed much more rapidly than reduction of **1** by common XEC reductants provide evidence against a mechanism in which (bpy)Ni⁰ intermediates activate electrophiles. Another contested mechanistic proposal in XEC reactions is the origin of cross-selectivity for C(sp²)-C(sp³) products over C(sp²)-C(sp²) or C(sp³)-C(sp³) coupling. Two major proposals on the origin of cross-selectivity have been made: (1) orthogonal activation of C(sp²)-X and C(sp³)-X electrophiles by (bpy)Ni^IX or (bpy)Ni^I(Ar), respectively, imparts selectivity on products,^{16,47} and (2) substrate activation need not be mediated by distinct Ni complexes, but product selectivity arises per the persistent radical effect, in which the rates at which (bpy)Ni^{II}(Ar)X (a persistent “metalloradical”) and alkyl radical (a transient radical) are generated must be matched.^{3,48}

In order to assess these proposals, we evaluated several C(sp²)-C(sp³) cross-couplings between an aryl halide and a primary alkyl halide for which we had gathered kinetic data on substrate activation by **1** in THF (Figure 7A). Based on our kinetic data, we designed two sets of XEC reactions in which the halide identity of one substrate was varied to give rate-matched and rate-mismatched cases. Furthermore, reactions were run in both THF and DMF to investigate solvent-dependent variations in the mechanism. In the first set of reactions studied (Reaction I), the halide identity of the

C(sp²)-X partner was varied. For the rate-matched substrate pairing—1-chloro-4-fluorobenzene and 1-bromo-3-phenylpropane—we observed cross-selectivity for the desired C(sp²)-C(sp³) cross-coupled product (**8**) in THF (entry 1). However, when switching the halide identity of the C(sp²)-X partner from chloride to bromide (a > 100-fold increase in activation rate by **1**), we observed only trace amounts of **8** and C(sp²)-C(sp²) homocoupling became the major pathway (entry 2). For the same XEC reactions in DMF, a more common solvent for XEC reactions,³ we observed an erosion in cross-selectivity for the aryl chloride coupling (entry 3) and a 5-fold improvement in cross-selectivity for the bromoarene coupling (entry 4).

In the second set of reactions studied (Reaction II), the halide identity of the C(sp³)-X partner was varied. In this case, the coupling between 4-chlorobenzotrifluoride and 1-iodo-3-phenylpropane is rate matched, and we observed excellent cross-selectivity for the desired C(sp²)-C(sp³) cross-coupled product (**9**) in THF (entry 5). In line with our kinetic data, the mismatched coupling with 1-bromo-3-phenylpropane afforded **9** in a decreased yield with poor cross-selectivity in THF (entry 6). However—as was observed in Reaction I—rate-matching based on kinetic observations in THF was no longer predictive for the yield of **9** for XECs in DMF (entries 7 and 8). In this case, the yield of **9** in the “mismatched” case in DMF even exceeds that in the matched case in THF.

We attribute the observed solvent-dependent reactivity to a change in the identity of the species activating the alkyl halide partner. In THF, we propose that **1** activates both electrophiles, with the persistent radical effect affording cross-selectivity (Figure 7B). Thus, kinetic data for substrate activation by **1** is predictive of XEC rate-matching in THF.

In DMF, **1** may activate the alkyl halide partner to some extent, but we propose that reduced species derived from (bpy)-Ni^{II}(Ar)X (herein, (bpy)Ni^I(Ar)) are also formed and react with the alkyl bromide partner to generate alkyl radicals, as previously studied by Diao and co-workers.¹⁶ Indeed, these observations are consistent with the reduction potentials for relevant (^t-Bu₃bpy)Ni^{II} species: the relative favorability for reduction of **3** and (^t-Bu₃bpy)Ni(*o*-Tol)Br are reversed in THF and DMF (Figure 7C).

Literature values indicate that XAA by (bpy)Ni^I(Ar) should proceed with larger rate constants than XAA by **1**,¹⁶ which helps account for the 5-fold increase in formation of **8** between entries 2 and 4 and the reversal of the expected cross-selectivity for **9** in entries 7 and 8. However, the data for Reaction I suggest that the more selective electrophile activation in DMF (i.e., ArBr is activated by **1**, alkyl bromide is activated by (bpy)Ni^I(Ar)) is not sufficient for obtaining cross-selectivity. We attempted to generate (bpy)Ni^I(Ar) species through transmetalation for in situ studies of activation rates, but we observed rapid disproportionation to **2** and (bpy)Ni^{II}(Ar)₂ that prevented further studies (see SI section 5.6 for further discussion).⁴⁹

Given these observations, we can propose a catalytic cycle for bpy/Ni-catalyzed XEC reactions that is consistent with our data (Figure 7B). Oxidative addition of the C(sp²)-X electrophile to a (bpy)Ni^IX species affords a (bpy)Ni^{II}(Ar)X intermediate after rapid disproportionation or reduction from a Ni^{III} oxidative adduct. Addition of an alkyl radical to this (bpy)Ni^{II}(Ar)X intermediate affords the C(sp²)-C(sp³) coupled product following reductive elimination from Ni^{III}.⁵⁰ The aforementioned alkyl radical can be generated by either a (bpy)Ni^IX species or a (bpy)Ni^I(Ar) species, depending on solvent identity (and perhaps other factors, such as the reducing agent). To achieve cross-selectivity, it is possible to have unselective electrophilic activation (e.g., **1** activating both substrates) if the rates of substrate activation are sufficiently matched. Furthermore, even for scenarios in which electrophile activation is mediated by distinct Ni species, rate matching of substrate activation still appears to be necessary to obtain cross-selectivity.

3. CONCLUSIONS

Catalytically relevant reactivity studies have been conducted on (^t-Bu₃bpy)Ni^I complex **1** and (^t-Bu₃bpy)Ni⁰ complex **2**. Overall, the large rate constants for C(sp²)-X oxidative addition to **1**, particularly for aryl bromides and iodides, relative to the other reactions studied suggest that (bpy)Ni^IX species are likely to react with aryl halides when they are substrates in catalytic reactions instead of other pathways. We also implicate the intermediacy of **1** in the reactions of aryl halides with **2**, which is likely a general phenomenon for (bpy)Ni⁰(olefin) species. We also demonstrate that (bpy)Ni^IX species are kinetically competent toward XAA of alkyl halides, complementing previous proposals based on the reactivity of (bisphosphine)-Ni^IX species.¹² Based on the observed rate constants, dimerization of **1** to give **4** does not appear to be competitive with reactions of **1** with substrates in a catalytic reaction. However, due to the low solubility of **4** and the irreversible nature of the dimerization, formation of **4** may occur in catalytic reactions depending on substrate and solvent identity. Our findings provide insights into additive and solvent selection that can be employed if catalyst deactivation due to aggregation is suspected.

Taken together, these data allow for an analysis of the mechanism and the origin of cross-selectivity in XEC reactions. We find that reduction of **1** to **2** with common metal reductants for XEC reactions is more inefficient than reactions between **1** and common electrophiles, suggesting that (bpy)Ni⁰ species are not easily generated under XEC conditions. Our data suggest that both (bpy)Ni^IX species and (bpy)Ni^I(Ar) species are capable of mediating XAA for XEC reactions, with solvent identity dictating which is the major pathway. In THF solution, where reduction of (bpy)Ni^{II}(Ar)X species is unfavorable, cross-selectivity could be achieved despite unselective activation by (bpy)Ni^IX for suitably rate-matched substrates. In DMF solution, where we propose substrate activation is more selective due to the increased favorability of (bpy)Ni^{II}(Ar)X reduction, the data indicate that rate matching of substrate activation remains necessary for obtaining satisfactory cross-selectivity.

We anticipate that these findings will inform mechanistic proposals, solvent and additive selections, and reaction design for future Ni-catalyzed cross-coupling reactions. Further investigations in this area should evaluate complexes bearing other nitrogen ligands (particularly chiral variants), mechanism-informed modeling, and precatalyst design.

■ ASSOCIATED CONTENT

Supporting Information

The Supporting Information is available free of charge at <https://pubs.acs.org/doi/10.1021/jacs.5c11247>.

Experimental procedures, experimental data, and characterization and spectral data for new compounds (PDF)

Accession Codes

Deposition Number 2465927 contains the supplementary crystallographic data for this paper. These data can be obtained free of charge via the joint Cambridge Crystallographic Data Centre (CCDC) and Fachinformationszentrum Karlsruhe Access Structures service.

■ AUTHOR INFORMATION

Corresponding Author

Abigail G. Doyle – Department of Chemistry and Biochemistry, University of California Los Angeles, Los Angeles, California 90095, United States; orcid.org/0000-0002-6641-0833; Email: abigaildoyle@ucla.edu

Author

T. Judah Raab – Department of Chemistry and Biochemistry, University of California Los Angeles, Los Angeles, California 90095, United States; orcid.org/0000-0001-9449-5574

Complete contact information is available at: <https://pubs.acs.org/10.1021/jacs.5c11247>

Notes

The authors declare no competing financial interest.

■ ACKNOWLEDGMENTS

Financial support was provided by NIGMS R35 GM126986. We thank Alex Cusumano, Erin Bucci, and Braden Chaffin for helpful discussions. These studies were supported by shared instrumentation grants from the National Science Foundation under equipment grants CHE-1048804 and 2117480, along

with the NIH Office of Research Infrastructure Program supergrant S10OD028644.

REFERENCES

- (1) Diccianni, J. B.; Diao, T. Mechanisms of Nickel-Catalyzed Cross-Coupling Reactions. *Trends Chem.* **2019**, *1*, 830–844.
- (2) Chan, A. Y.; Perry, I. B.; Bissonnette, N. B.; Buksh, B. F.; Edwards, G. A.; Frye, L. I.; Garry, O. L.; Lavagnino, M. N.; Li, B. X.; Liang, Y.; Mao, E.; Millet, A.; Oakley, J. V.; Reed, N. L.; Sakai, H. A.; Seath, C. P.; MacMillan, D. W. C. Metallaphotoredox: The Merger of Photoredox and Transition Metal Catalysis. *Chem. Rev.* **2022**, *122*, 1485–1542.
- (3) Ehehalt, L. E.; Beleh, O. M.; Priest, I. C.; Mouat, J. M.; Olszewski, A. K.; Ahern, B. N.; Cruz, A. R.; Chi, B. K.; Castro, A. J.; Kang, K.; Wang, J.; Weix, D. J. Cross-Electrophile Coupling: Principles, Methods, and Applications in Synthesis. *Chem. Rev.* **2024**, *124*, 13397–13569.
- (4) Cagan, D. A.; Bim, D.; Kazmierczak, N. P.; Hadt, R. G. Mechanisms of Photoredox Catalysis Featuring Nickel-Bipyridine Complexes. *ACS Catal.* **2024**, *14*, 9055–9076.
- (5) Lin, Q.; Spielvogel, E. H.; Diao, T. Carbon-Centered Radical Capture at Nickel(II) Complexes: Spectroscopic Evidence, Rates, and Selectivity. *Chem.* **2023**, *9*, 1295–1308.
- (6) Spielvogel, E. H.; Yuan, J.; Hoffmann, N. M.; Diao, T. Nickel-Mediated Radical Capture: Evidence for a Concerted Inner-Sphere Mechanism. *J. Am. Chem. Soc.* **2025**, *147*, 19632–19642.
- (7) Mohadjer Beromi, M.; Brudvig, G. W.; Hazari, N.; Lant, H. M. C.; Mercado, B. Q. Synthesis and Reactivity of Paramagnetic Nickel Polypyridyl Complexes Relevant to C(sp²)-C(sp³) Coupling Reactions. *Angew. Chem., Int. Ed.* **2019**, *58*, 6094–6098.
- (8) Cagan, D. A.; Bim, D.; McNicholas, B. J.; Kazmierczak, N. P.; Oyala, P. H.; Hadt, R. G. Photogenerated Ni(I)-Bipyridine Halide Complexes: Structure-Function Relationships for Competitive C(sp²)-Cl Oxidative Addition and Dimerization Reactivity Pathways. *Inorg. Chem.* **2023**, *62*, 9538–9551.
- (9) Ting, S. L.; Williams, W. L.; Doyle, A. G. Oxidative Addition of Aryl Halides to a Ni(I)-Bipyridine Complex. *J. Am. Chem. Soc.* **2022**, *144*, 5575–5582.
- (10) Anghileri, L.; Baunis, H.; Bena, A. R.; Giannoudis, C.; Burke, J. H.; Reischauer, S.; Merschjann, C.; Wallick, R. F.; Al Said, T.; Adams, C. E.; Simionato, G.; Kovalenko, S.; Dell'Amico, L.; van der Veen, R. M.; Pieber, B. Evidence for a Unifying Ni^I/Ni^{III} Mechanism in Light-Mediated Cross-Coupling Catalysis. *J. Am. Chem. Soc.* **2025**, *147*, 13169–13179.
- (11) Akana, M. E.; Tcyrulnikov, S.; Akana-Schneider, B. D.; Reyes, G. P.; Monfette, S.; Sigman, M. S.; Hansen, E. C.; Weix, D. J. Computational Methods Enable the Prediction of Improved Catalysts for Nickel-Catalyzed Cross-Electrophile Coupling. *J. Am. Chem. Soc.* **2024**, *146*, 3043–3051.
- (12) Diccianni, J. B.; Katigbak, J.; Hu, C.; Diao, T. Mechanistic Characterization of (Xantphos)Ni(I)-Mediated Alkyl Bromide Activation: Oxidative Addition, Electron Transfer, or Halogen-Atom Abstraction. *J. Am. Chem. Soc.* **2019**, *141*, 1788–1796.
- (13) Anderson, T. J.; Jones, G. D.; Vivic, D. A. Evidence for a Ni^I Active Species in the Catalytic Cross-Coupling of Alkyl Electrophiles. *J. Am. Chem. Soc.* **2004**, *126*, 8100–8101.
- (14) Schley, N. D.; Fu, G. C. Nickel-Catalyzed Negishi Arylations of Propargylic Bromides: A Mechanistic Investigation. *J. Am. Chem. Soc.* **2014**, *136*, 16588–16593.
- (15) Turro, R. F.; Wahlman, J. L. H.; Tong, Z. J.; Chen, X.; Yang, M.; Chen, E. P.; Hong, X.; Hadt, R. G.; Houk, K. N.; Yang, Y.-F.; Reisman, S. E. Mechanistic Investigation of Ni-Catalyzed Reductive Cross-Coupling of Alkenyl and Benzyl Electrophiles. *J. Am. Chem. Soc.* **2023**, *145*, 14705–14715.
- (16) Lin, Q.; Fu, Y.; Liu, P.; Diao, T. Monovalent Nickel-Mediated Radical Formation: A Concerted Halogen-Atom Dissociation Pathway Determined by Electroanalytical Studies. *J. Am. Chem. Soc.* **2021**, *143*, 14196–14206.
- (17) Newman-Stonebraker, S. H.; Raab, T. J.; Roshandel, H.; Doyle, A. G. Synthesis of Nickel(I)-Bromide Complexes via Oxidation and Ligand Displacement: Evaluation of Ligand Effects on Speciation and Reactivity. *J. Am. Chem. Soc.* **2023**, *145*, 19368–19377.
- (18) Inatomi, T.; Fukahori, Y.; Yamada, Y.; Ishikawa, R.; Kanegawa, S.; Koga, Y.; Matsubara, K. Ni(I)-Ni(III) Cycle in Buchwald-Hartwig Amination of Aryl Bromide Mediated by NHC-Ligated Ni(I) Complexes. *Catal. Sci. Technol.* **2019**, *9*, 1784–1793.
- (19) Huang, H.; Alvarez-Hernandez, J. L.; Hazari, N.; Mercado, B. Q.; Uehling, M. R. Effect of 6,6'-Substituents on Bipyridine-Ligated Ni Catalysts for Cross-Electrophile Coupling. *ACS Catal.* **2024**, *14*, 6897–6914.
- (20) Johnson Humphrey, E. L. B.; Kennedy, A. R.; Sproules, S.; Nelson, D. J. Evaluating a Dispersion of Sodium in Sodium Chloride for the Synthesis of Low-Valent Nickel Complexes. *Eur. J. Inorg. Chem.* **2022**, No. e202101006.
- (21) Till, N. A.; Oh, S.; MacMillan, D. W. C.; Bird, M. J. The Application of Pulse Radiolysis to the Study of Ni(I) Intermediates in Ni-Catalyzed Cross-Coupling Reactions. *J. Am. Chem. Soc.* **2021**, *143*, 9332–9337.
- (22) Dawson, G. A.; Lin, Q.; Neary, M. C.; Diao, T. Ligand Redox Activity of Organonickel Radical Complexes Governed by the Geometry. *J. Am. Chem. Soc.* **2023**, *145*, 20551–20561.
- (23) Tolman, C. A.; Seidel, W. C.; Gosser, L. W. Formation of Three-Coordinate Nickel(0) Complexes by Phosphorus Ligand Dissociation from NiL₄. *J. Am. Chem. Soc.* **1974**, *96*, 53–60.
- (24) Solodar, J.; Petrovich, J. P. Behavior of Silver(I)-Olefin Complexes in Organic Media. *Inorg. Chem.* **1971**, *10*, 395–397.
- (25) Cagan, D. A.; Bim, D.; Silva, B.; Kazmierczak, N. P.; McNicholas, B. J.; Hadt, R. G. Elucidating the Mechanism of Excited-State Bond Homolysis in Nickel-Bipyridine Photoredox Catalysts. *J. Am. Chem. Soc.* **2022**, *144*, 6516–6531.
- (26) Sutcliffe, E.; Cagan, D. A.; Hadt, R. G. Ultrafast Photophysics of Ni(I)-Bipyridine Halide Complexes: Spanning the Marcus Normal and Inverted Regimes. *J. Am. Chem. Soc.* **2024**, *146*, 15506–15514.
- (27) Indelli, M. T.; Ghirelli, M.; Prodi, A.; Chiorboli, C.; Scandola, F.; McClenaghan, N. D.; Puntoriero, F.; Campagna, S. Solvent Switching of Intramolecular Energy Transfer in Bichromophoric Systems: Photophysics of (2,2'-Bipyridine)Tetracyanoruthenate(II)/Pyrenyl Complexes. *Inorg. Chem.* **2003**, *42*, 5489–5497.
- (28) [(^tBu₂ppy)NiBr]₂ absorbs broadly in the visible region and exhibits low solubility in organic solvents, which may lead to scattering upon precipitation. Taken together, these factors likely lead to a deflation in the observed k₅ values.
- (29) Prieto Kullmer, C. N.; Kautzky, J. A.; Krska, S. W.; Nowak, T.; Dreher, S. D.; MacMillan, D. W. C. Accelerating Reaction Generality and Mechanistic Insight through Additive Mapping. *Science* **2022**, *376*, 532–539.
- (30) Till, N. A.; Tian, L.; Dong, Z.; Scholes, G. D.; MacMillan, D. W. C. Mechanistic Analysis of Metallaphotoredox C-N Coupling: Photocatalysis Initiates and Perpetuates Ni(I)/Ni(III) Coupling Activity. *J. Am. Chem. Soc.* **2020**, *142*, 15830–15841.
- (31) Kawamata, Y.; Vantourout, J. C.; Hickey, D. P.; Bai, P.; Chen, L.; Hou, Q.; Qiao, W.; Barman, K.; Edwards, M. A.; Garrido-Castro, A. F.; deGruyter, J. N.; Nakamura, H.; Knouse, K.; Qin, C.; Clay, K. J.; Bao, D.; Li, C.; Starr, J. T.; Garcia-Irizarry, C.; Sach, N.; White, H. S.; Neurock, M.; Minter, S. D.; Baran, P. S. Electrochemically Driven, Ni-Catalyzed Aryl Amination: Scope, Mechanism, and Applications. *J. Am. Chem. Soc.* **2019**, *141*, 6392–6402.
- (32) Sun, R.; Qin, Y.; Rucolo, S.; Schnedermann, C.; Costentin, C.; Nocera, D. G. Elucidation of a Redox-Mediated Reaction Cycle for Nickel-Catalyzed Cross Coupling. *J. Am. Chem. Soc.* **2019**, *141*, 89–93.
- (33) Biscoe, M. R.; Fors, B. P.; Buchwald, S. L. A New Class of Easily Activated Palladium Precatalysts for Facile C–N Cross-Coupling Reactions and the Low Temperature Oxidative Addition of Aryl Chlorides. *J. Am. Chem. Soc.* **2008**, *130*, 6686–6687.

(34) The proposal that aryl chloride oxidative addition to **1** proceeds via an S_NAr -type mechanism likely originates from a Hammett plot in which $\ln(k_X/k_H)$ was plotted vs. σ rather than $\log(k_X/k_H)$. This led to a ρ value of +5.2 instead of the ρ of +2.3 that would have otherwise been obtained.

(35) Wu, T.; Castro, A. J.; Ganguli, K.; Rotella, M. E.; Ye, N.; Gallou, F.; Wu, B.; Weix, D. J. Cross-Electrophile Coupling to Form Sterically Hindered C(Sp²)–C(Sp³) Bonds: Ni and Co Afford Complementary Reactivity. *J. Am. Chem. Soc.* **2025**, *147*, 9449–9456.

(36) Mullins, R. J.; Vedernikov, A.; Viswanathan, R. Competition Experiments as a Means of Evaluating Linear Free Energy Relationships. An Experiment for the Advanced Undergraduate Organic Chemistry Lab. *J. Chem. Educ.* **2004**, *81*, 1357.

(37) Fristrup, P.; Le Quement, S.; Tanner, D.; Norrby, P. O. Reactivity and Regioselectivity in the Heck Reaction: Hammett Study of 4-Substituted Styrenes. *Organometallics* **2004**, *23*, 6160–6165.

(38) Pérez–García, P. M.; Darù, A.; Scheerder, A. R.; Lutz, M.; Harvey, J. N.; Moret, M. E. Oxidative Addition of Aryl Halides to a Triphosphine Ni(0) Center to Form Pentacoordinate Ni(II) Aryl Species. *Organometallics* **2020**, *39*, 1139–1144.

(39) Pierson, C. N.; Hartwig, J. F. Mapping the Mechanisms of Oxidative Addition in Cross-Coupling Reactions Catalysed by Phosphine-Ligated Ni(0). *Nat. Chem.* **2024**, *16*, 930–937.

(40) Day, C. S.; Rentería-Gómez, A.; Ton, S. J.; Gogoi, A. R.; Gutierrez, O.; Martin, R. Elucidating Electron-Transfer Events in Polypyridine Nickel Complexes for Reductive Coupling Reactions. *Nat. Catal.* **2023**, *6*, 244–253.

(41) Shields, B. J.; Kudisch, B.; Scholes, G. D.; Doyle, A. G. Long-Lived Charge Transfer States of Nickel(II) Aryl Halide Complexes Facilitate Bimolecular Photoinduced Electron Transfer. *J. Am. Chem. Soc.* **2018**, *140*, 3035–3039.

(42) Derosa, J.; Apolinar, O.; Kang, T.; Tran, V. T.; Engle, K. M. Recent Developments in Nickel-Catalyzed Intermolecular Dicarbofunctionalization of Alkenes. *Chem. Sci.* **2020**, *11*, 4287–4296.

(43) Sun, R.; Qin, Y.; Nocera, D. G. General Paradigm in Photoredox Nickel-Catalyzed Cross-Coupling Allows for Light-Free Access to Reactivity. *Angew. Chem., Int. Ed.* **2020**, *59*, 9527–9533.

(44) Greaves, M. E.; Ronson, T. O.; Lloyd-Jones, G. C.; Maseras, F.; Sproules, S.; Nelson, D. J. Unexpected Nickel Complex Speciation Unlocks Alternative Pathways for the Reactions of Alkyl Halides with Dppf-Nickel(0). *ACS Catal.* **2020**, *10*, 10717–10725.

(45) In the case of 1-iodo-3-phenylpropane, a change in the order of [1] was observed, which we attribute to rate-limiting radical capture following halogen atom abstraction.

(46) Su, Z.-M.; Deng, R.; Stahl, S. S. Zinc and Manganese Redox Potentials in Organic Solvents and Their Influence on Nickel-Catalysed Cross-Electrophile Coupling. *Nat. Chem.* **2024**, *16*, 2036–2043.

(47) Dawson, G. A.; Spielvogel, E. H.; Diao, T. Nickel-Catalyzed Radical Mechanisms: Informing Cross-Coupling for Synthesizing Non-Canonical Biomolecules. *Acc. Chem. Res.* **2023**, *56*, 3640–3653.

(48) Leifert, D.; Studer, A. The Persistent Radical Effect in Organic Synthesis. *Angew. Chem., Int. Ed.* **2020**, *59*, 74–108.

(49) Romero-Arenas, A.; Popescu, M. V.; Goetz, M. K.; Bhatnagar, R.; Goljani, H.; Punchihewa, B. T.; Sanders, K. M.; Guzei, I. A.; Rafiee, M.; Weix, D. J.; Paton, R. S.; Stahl, S. S. Reductively Induced Aryl Transmetalation: An Alternative Catalytically Relevant Ni-Catalyzed Biaryl Coupling Mechanism. *J. Am. Chem. Soc.* **2025**, *147*, 21697–21707.

(50) Recent work from Diao and coworkers (ref. 6) has suggested that radical addition and reductive elimination may not be stepwise but instead a concerted process. It is unclear whether this mechanism is operative from our study.